

# Blue Luminescent Organoaluminum Compounds: Al(CH<sub>3</sub>)<sub>2</sub>(dpa), Al<sub>2</sub>(CH<sub>3</sub>)<sub>5</sub>(dpa)<sub>2</sub>, Al<sub>4</sub>(O)<sub>2</sub>(CH<sub>3</sub>)<sub>6</sub>(dpa)<sub>2</sub>, and Al(pfap)<sub>3</sub>, dpa = Deprotonated Di-2-pyridylamine, pfap = Deprotonated 2-Pentafluoroanilinopyridine

James Ashenurst,<sup>†</sup> Lorenzo Brancalon,<sup>‡</sup> Shu Gao,<sup>†</sup> Wang Liu,<sup>†</sup>  
Hartmut Schmider,<sup>†</sup> Suning Wang,<sup>\*,†</sup> Gang Wu,<sup>†</sup> and Q. G. Wu<sup>†</sup>

Department of Chemistry, Queen's University, Kingston, Ontario, K7L 3N6 Canada, and  
Steacie Institute for Molecular Science, National Research Council, 100 Sussex Drive,  
Ottawa, Ontario, K1N 0R6 Canada

Received June 24, 1998

The reactions of Al(CH<sub>3</sub>)<sub>3</sub> with di-2-pyridylamine (dpaH) yielded a mononuclear zwitterion complex, Al(CH<sub>3</sub>)<sub>2</sub>(dpa) (**1**), a dinuclear complex, Al<sub>2</sub>(CH<sub>3</sub>)<sub>5</sub>(dpa) (**2**), and a tetranuclear complex, Al<sub>4</sub>(O)<sub>2</sub>(CH<sub>3</sub>)<sub>6</sub>(dpa)<sub>2</sub> (**3**), depending on the stoichiometry and conditions of the reactions. The crystal structures of all three compounds were determined by single-crystal X-ray diffraction analyses. All three compounds emit an intense blue color in solution and the solid state at  $\lambda_{\max}$  = 475, 445, and 450 nm, respectively, when irradiated by an UV light. Molecular orbital calculations using ab initio methods (Gaussian 94) on dpa, dpaH, and compound **1** were performed which revealed that the aluminum ion in compounds **1–3** plays a key role in stabilizing the complexes and promoting the blue luminescence. The reaction of Al(CH<sub>3</sub>)<sub>3</sub> with 2-pentafluoroanilinopyridine (pfapH) resulted in the formation of a mononuclear octahedral complex, Al(pfap)<sub>3</sub> (**4**). Variable-temperature and COSY <sup>1</sup>H NMR established that compound **4** is highly fluxional in solution due to a rapid interconversion of *mer* and *fac* isomers, with the *mer* isomer dominating at low temperature. The structure of the *fac* isomer of **4** was determined by X-ray diffraction. Compound **4** emits at  $\lambda_{\max}$  = 409 nm when irradiated by an UV light.

## Introduction

Blue luminescent compounds have attracted much attention recently because of their various applications in material science, the most attractive of which is as blue emitters in full-color electroluminescent displays.<sup>1–4</sup> There are essentially three classes of blue emitters in

electroluminescent displays: inorganic semiconductors, organic polymers, and small organic/organometallic molecules. Devices made of inorganic semiconductors are very costly to produce and often suffer from low efficiency. Organic polymers have the inherent weaknesses of low purity and poor stability, which often result in the poor performance of the device. The major advantage of small organic/organometallic compounds over inorganic semiconductors or organic polymers is that they could be vacuum-deposited readily so that the fabrication of high-quality EL devices could be achieved readily and cost-effectively. The commercialization of full-color flat panel displays based on electroluminescence of small molecules has been hindered by the lack of efficient and stable blue emitters. We believe that organometallic complexes could play a key role in the development of electroluminescent displays because one could tune the emission color, volatility, and stability of the complex readily by manipulating the ligand and the coordination environment around the central atom. The previously known blue luminescent organometallic complexes that have only limited applications in EL displays are either 8-hydroxyquinoline- or azomethine-based complexes where either aluminum or zinc ions are involved.<sup>4</sup> The 8-hydroxyquinoline complexes typically emit in the yellow-green region. To achieve blue luminescent 8-hydroxyquinoline complexes, an elaborate modification of the 8-hydroxyquinoline ligand is necessary, which limits the practical application of

<sup>†</sup> Queen's University.

<sup>‡</sup> National Research Council of Canada.

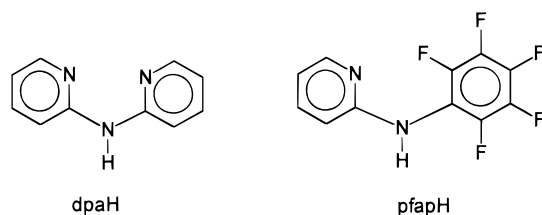
(1) Trepanier, S. J.; Wang, S. *Organometallics* **1996**, *15*, 760. (b) Trepanier, S. J.; Wang, S. *Can. J. Chem.* **1996**, *74*, 2032. (c) Trepanier, S. J.; Wang, S. *J. Chem. Soc., Dalton Trans.* **1995**, 2425. (d) Trepanier, S. J.; Wang, S. *Angew. Chem., Int. Ed. Engl.* **1994**, *33*, 1265.

(2) Rack, P. D.; Naman, A.; Holloway, P. H.; Sun, S.; Tuenge, R. T. *Mater. Res. Bull.* **1996**, *21* (3), 49. (b) Sze, S. M. *Physics of Semiconductor Devices*; Wiley: New York, 1981. (c) Mauch, R. H.; Velthaus, K.-O.; Hüttel, B.; Troppenz, U.; Herrmann, R. *Society for Information Displays, 95 Digest*, **1995**, 720. (d) Sun, S. S.; Tuenge, R. T.; Kane, J.; Ling, M. *J. Electrochem. Soc.* **1994**, *141* (10), 2877.

(3) Pei, Q.; Yu, G.; Zhang, C.; Yang, Y.; Heeger, A. J. *Science* **1995**, *269*, 1086. (b) Yang, Y. *Polymer Electroluminescent Devices*. In *Mater. Res. Soc. Bull.* **1997**, *22* (6), 31. (c) Tsutsui, T. *Progress in Electroluminescent Devices Using Molecular Thin Films*. In *Mater. Res. Soc. Bull.* **1997**, *22* (6), 39. (d) Brouwer, H. J.; Krasnikov, V. V.; Hilberer, A.; Hadziioannou, G. *Adv. Mater.* **1996**, *8*, 935. (e) Edwards, A.; Blumstengel, S.; Sokolik, I.; Dorsinville, R.; Yun, H.; Kwei, K.; Okamoto, Y. *Appl. Phys. Lett.* **1997**, *70*, 298. (f) Ohmori, Y.; Uchida, M.; Muro, K.; Yoshino, K. *Jpn. J. Appl. Phys.* **1991**, *30*, L1941.

(4) Moore, C. P.; VanSlyke, S. A.; Gysling, H. J. US Patent, No. 5484922, 1996. (b) Sano, T.; Fujita, M.; Fujii, T.; Nishio, Y.; Hamada, Y.; Shibata, K.; Kuroki, K. US Patent, No. 5432014, 1995. (c) Hironaka, Y.; Nakamura, H.; Kusumoto, T. US Patent, No. 5466392, 1995. (d) VanSlyke, S. A.; Bryan, P. S.; Lovecchio, F. V. US Patent, No. 5150006, 1992. (e) Bryan, P. S.; Lovecchio, F. V.; VanSlyke, S. A. US Patent, No. 5141671, 1992. (f) Hamada, Y.; Sano, T.; Fujita, M.; Fujii, T.; Nishio, Y.; Shibata, K. *Chem. Lett.* **1993**, 905. (g) Nakamura, N.; Wakabayashi, S.; Miyairi, K.; Fujii, T. *Chem. Lett.* **1994**, 1741.

Chart 1. dpaH and pfapH Ligands



8-hydroxyquinoline-based complexes. We therefore initiated the search for new blue luminescent organometallic compounds. Our first goal was to find new ligands that when bound to Al(III) or B(III) produce blue luminescence. Ultimately we want to produce stable and efficient blue luminescent compounds based on the new ligand systems and investigate their electroluminescent performance. In two recent preliminary communication articles,<sup>5</sup> we reported that 7-azaindole and di-2-pyridylamine produce blue luminescence when deprotonated and bound to either an Al(III) or B(III) center. A complete account on the 7-azaindole-based blue luminescent aluminum compounds has been given in two recent full papers.<sup>6</sup> Herein we give a detailed account of syntheses, structures, and photoluminescent properties of aluminum complexes based on di-2-pyridylamine and 2-pentafluoroanilinopyridine ligands (Chart 1).

### Experimental Section

All reactions were carried out under a nitrogen atmosphere using either the standard Schlenk line techniques or the inert atmosphere drybox.  $\text{Al}(\text{CH}_3)_3$  and di-2-pyridylamine were purchased from Aldrich Chemical Co. 2-Pentafluoroanilinopyridine was synthesized according to the method of Koppang.<sup>7</sup> Solvents were freshly distilled from the appropriate drying agents under nitrogen.  $^1\text{H}$  NMR spectra were recorded on either a Bruker AM 400 or a Bruker ACF 200 spectrometer. The 2D COSY experiment was performed at 243 K on a Bruker AM400 spectrometer. A total of 512  $t_1$  increments were acquired and zero-filled to 1024 in the  $t_1$  dimension prior to the 2D Fourier transformation (2D FT). For each  $t_1$ , 16 scans were accumulated. Sine-bell window functions were applied in both dimensions. The spectral width was 1000 Hz. The total time to record the 2D free-induction-decay (FID) was about 4.6 h. Elemental analyses were performed by Canadian Microanalytical Service, Delta, British Columbia. Excitation and emission spectra were recorded on Photon Technologies International QM1 spectrometer. The quantum yield and emission lifetime were measured on a Time Master spectrometer of Photon Technologies International. The time-resolved measurements were recorded with the method of single-photon counting. NaX zeolite was used to record the lamp profile. The sample was placed at  $45^\circ$  to both excitation and emission beams.

**Synthesis of  $\text{Al}(\text{CH}_3)_2(\text{dpa})$  (1).** To 342 mg (0.002 mol) of di-2-pyridylamine in 5 mL toluene was added 1 mL (0.002 mol) of  $\text{Al}(\text{CH}_3)_3$  (2.0 M in toluene), turning the solution bright yellow. The mixture was stirred for 3 h and concentrated to  $\sim 2$  mL by vacuum. Pale yellow thin plate crystals of **1** were obtained in 61% yield after standing overnight at ambient temperature.  $^1\text{H}$  NMR ( $\delta$ ,  $\text{CDCl}_3$ , ppm, 298 K):  $-0.65$  (s, 6H,

$\text{CH}_3$ ), 6.65 ( $t$ , 2H, dpa), 7.00 ( $d$ , 2H, dpa), 7.51 ( $t$ , 2H, dpa), 7.63 ( $d$ , 2H, dpa).  $^{13}\text{C}$  NMR ( $\delta$ ,  $\text{CDCl}_3$ , ppm, 298 K):  $-10.00$  (br, Al- $\text{CH}_3$ ), 112.93, 124.10, 139.14, 140.22, 158.23 (dpa). Anal. Calcd for **1**,  $\text{C}_{12}\text{H}_{14}\text{AlN}_3$ : C, 63.43; H, 6.21; N, 18.49. Found: C, 62.81; H, 5.98; N, 18.55.

**Synthesis of  $\text{Al}_2(\text{CH}_3)_5(\text{dpa})$  (2).** To 516 mg (0.003 mol) of di-2-pyridylamine in 10 mL toluene was added 3 mL (0.006 mol) of  $\text{Al}(\text{CH}_3)_3$  (2.0 M in toluene). Upon addition of  $\text{Al}(\text{CH}_3)_3$  the mixture became bright yellow, then clear. After stirring for 3 h, the solution was concentrated to  $\sim 4$  mL under vacuum. Large, colorless crystals of **2** formed after 2 days in 70% yield.  $^1\text{H}$  NMR ( $\delta$ ,  $\text{CDCl}_3$ , 298 K):  $-0.93$  (s, 9H,  $\text{CH}_3$ ),  $-0.57$  (s, 6H,  $\text{CH}_3$ ), 7.05 ( $t$ , 2H, dpa), 7.53 ( $d$ , 2H, dpa), 7.80 ( $t$ , 2H, dpa), 7.92 ( $d$ , 2H, dpa).  $^{13}\text{C}$  NMR ( $\delta$ ,  $\text{CDCl}_3$ , 213 K):  $-20.99$ ,  $-12.20$ ,  $-6.36$  (Al- $\text{CH}_3$ ); 117.63, 123.05, 140.86, 158.51 (dpa). Anal. Calcd for **2**,  $\text{C}_{15}\text{H}_{23}\text{Al}_2\text{N}_3$ : C, 60.21; H, 7.69; N, 14.05. Found: C, 59.27; H, 7.63; N, 13.93. Compound **2** was analyzed four times by using different batches of crystals sealed under vacuum. The results showed consistently a low carbon content, which could be a result of the high air-sensitivity of the compound. Similar phenomena have been observed previously.<sup>8</sup>

**Synthesis of  $\text{Al}_4(\text{CH}_3)_6(\text{O})_2(\text{dpa})_2$  (3).**  $\text{Al}(\text{CH}_3)_3$  (2.0 M, 1 mL, 2.0 mmol) in hexane was added to a 10 mL of toluene solution containing di-2-pyridylamine (0.17 g, 1.0 mmol) under nitrogen. After 30 min, 0.10 mL of unpurified dimethylformamide was added. The mixture was stirred for 6 h and filtered. Colorless crystals of **3** were obtained from the concentrated solution in 42% yield. (Compound **3** may also be obtained by passing a water-vapor saturated nitrogen through the reaction mixture.)  $^1\text{H}$  NMR ( $\delta$ , toluene- $d_7$ , ppm, 298 K):  $-0.53$  (s, 3H,  $\text{CH}_3$ ),  $-0.33$  (s, 3H,  $\text{CH}_3$ ),  $-0.13$  (s, 3H,  $\text{CH}_3$ ), 6.09 ( $t$ , 1H, 7-azain), 6.22 ( $qua$ , 1H, Py), 6.43 ( $d$ , 1H, Py), 6.74 ( $d$ , 1H, Py), 6.83 ( $m$ , 1H, Py), 6.90 ( $m$ , 1H, Py), 7.96 ( $d$ , 1H, Py), 8.26 ( $d$ , 1H, Py).  $^{13}\text{C}$  NMR ( $\delta$ ,  $\text{CDCl}_3$ , ppm, 298 K): 111.53, 112.85, 116.44, 137.75, 147.84 (dpa). (Not all resonances of dpa were observed due to the poor solubility of the compound. Al- $\text{CH}_3$  resonances were not observed due to both the poor solubility of the compound and the broadness of the peaks.) Anal. Calcd for **3**,  $\text{C}_{26}\text{H}_{34}\text{Al}_4\text{N}_6\text{O}_2/\text{C}_7\text{H}_8$ : C, 59.82; H, 6.34; N, 12.69. Found: C, 60.21; H, 6.25; N, 13.29. Mp: 165  $^\circ\text{C}$ .

**Synthesis of  $\text{Al}(\text{pfap})_3$  (4).** To the solution of 2-pentafluoroanilinopyridine (0.156 g, 0.60 mmol) in 5 mL of toluene was added  $\text{Al}(\text{CH}_3)_3$  (0.10 mL of a 2.0 M solution in hexane, 0.20 mmol) at ambient temperature. After being stirred overnight, the mixture was concentrated to about 1 mL by vacuum. Colorless crystals of **4** were obtained after a few days standing at ambient temperature. Yield: 0.126 g (78%).  $^1\text{H}$  NMR ( $\delta$ ,  $\text{CDCl}_3$ , 298 K): 6.20 ( $br$ , 1H), 6.44 ( $br$ ,  $t$ , 1H), 7.48 ( $br$ ,  $t$ , 1H), 7.70 ( $br$ , 1H). Anal. Calcd for  $\text{C}_3\text{H}_2\text{N}_6\text{F}_5\text{Al}$ : C, 49.27; H, 1.50; N, 10.45. Found: C, 48.88; H, 1.66; N, 10.44. Mp:  $> 280$   $^\circ\text{C}$ .

**X-ray Diffraction Analyses.** All crystals were obtained either from concentrated toluene solutions or from the solutions of toluene/hexane. The crystals were sealed in glass capillaries under nitrogen. All data were collected on a Siemens P4 single-crystal diffractometer with graphite-monochromated Mo K $\alpha$  radiation, operating at 50 kV and 40 mA at 23  $^\circ\text{C}$ . The data for **1** and **2** were collected over  $2\theta$  3–50 $^\circ$ , while the data for **3** and **4** were collected over  $2\theta$  3–45 $^\circ$  and 3–47 $^\circ$ , respectively. Three standard reflections were measured every 197 reflections. No significant decay was observed for all samples. Data were processed on a Pentium PC using Siemens SHELXTL software package<sup>9</sup> (version 5.0) and cor-

(5) Liu, W.; Hassan, A.; Wang, S. *Organometallics* **1997**, *16*, 4257.

(b) Hassan, A.; Wang, S. *J. Chem. Soc., Chem. Commun.* **1998**, 211.

(6) Ashenhurst, J.; Brancalion, L.; Hassan, A.; Liu, W.; Schmider, H.; Wang, S.; Wu, Q. *Organometallics* **1998**, *17*, 3186. (b) Gao, S.; Wu, Q.; Wu, G.; Wang, S. *Ibid.*, in press.

(7) Koppang, R. *J. Organomet. Chem.* **1972**, *46*, 193.

(8) Choquette, D. M.; Timm, M. J.; Hobbs, J. L.; Rahim, M.; Ahmed, K. J.; Planalp, R. P. *Organometallics* **1992**, *11*, 529. (b) Janik, J. F.; Duesler, E. N.; Paine, R. T. *Inorg. Chem.* **1987**, *26*, 4341. (c) Trepanier, S. J.; Wang, S. *Organometallics* **1994**, *13*, 2213. (d) Trepanier, S. J.; Wang, S. *J. Chem. Soc., Dalton Trans.* **1995**, 2425.

(9) SHELXTL crystal structure analysis package, Version 5; Bruker AXS, Analytical X-ray System: Madison, WI, 1995.

Table 1. Crystallographic Data

	1	2	3	4
formula	C <sub>12</sub> H <sub>14</sub> N <sub>3</sub> Al	C <sub>15</sub> H <sub>23</sub> N <sub>3</sub> Al <sub>2</sub>	C <sub>26</sub> H <sub>34</sub> N <sub>6</sub> O <sub>2</sub> Al <sub>4</sub> /C <sub>7</sub> H <sub>8</sub>	C <sub>33</sub> H <sub>12</sub> N <sub>6</sub> F <sub>15</sub> Al
fw	227.24	299.32	662.65	804.47
space group	<i>Pbca</i>	<i>P</i> $\bar{1}$	<i>P2</i> <sub>1</sub> / <i>c</i>	<i>Pbca</i>
<i>a</i> (Å)	7.040(2)	10.622(2)	8.725(2)	10.375(7)
<i>b</i> (Å)	12.470(2)	11.064(2)	14.158(3)	20.313(7)
<i>c</i> (Å)	28.038(3)	16.351(6)	14.994(3)	30.393(10)
$\alpha$ (deg)	90	103.49(2)	90	90
$\beta$ (deg)	90	98.30(2)	102.15(3)	90
$\gamma$ (deg)	90	93.825(7)	90	90
<i>V</i> (Å <sup>3</sup> )	2461.6(9)	1838.7(8)	1810.7(6)	6406(5)
<i>Z</i>	8	4	2	8
<i>D</i> <sub>c</sub> (g cm <sup>-3</sup> )	1.23	1.08	1.22	1.67
<i>T</i> (°C)	23	23	23	23
radiation, $\lambda$ (Å)	Mo K $\alpha$ , 0.710 73	Mo K $\alpha$ , 0.710 73	Mo K $\alpha$ , 0.710 73	Mo K $\alpha$ , 0.710 73
$\mu$ (cm <sup>-1</sup> )	1.41	1.53	1.66	1.88
final <i>R</i> [ <i>I</i> > 2 $\sigma$ ( <i>I</i> )]	<i>R</i> 1 <sup>a</sup> = 0.0509 w <i>R</i> 2 <sup>b</sup> = 0.1413	<i>R</i> 1 = 0.0472 w <i>R</i> 2 = 0.1121	<i>R</i> 1 = 0.0525 w <i>R</i> 2 = 0.1325	<i>R</i> 1 = 0.0770 w <i>R</i> 2 = 0.1643
<i>R</i> (all data)	<i>R</i> 1 = 0.0584 w <i>R</i> 2 = 0.1432	<i>R</i> 1 = 0.0888 w <i>R</i> 2 = 0.1396	<i>R</i> 1 = 0.0753 w <i>R</i> 2 = 0.1421	<i>R</i> 1 = 0.1744 w <i>R</i> 2 = 0.2259

$$^a R1 = \sum |F_o| - |F_c| / \sum |F_o|. \quad ^b wR2 = [\sum w[(F_o^2 - F_c^2)^2] / \sum [w(F_o^2)]]^{1/2}. \quad w = 1/[\sigma^2(F_o^2) + (0.075P)^2], \quad \text{where } P = [\max(F_o^2, 0) + 2F_c^2]/3.$$

rected for Lorentz and polarization effects. Neutral atom scattering factors were taken from Cromer and Waber.<sup>10</sup> The crystals of **1** and **4** belong to the orthorhombic space group *Pbca*, while the crystals of **3** belong to the monoclinic space group *P2*<sub>1</sub>/*c*, uniquely determined by systematic absences. Crystals of **2** belong to the triclinic space group *P* $\bar{1}$ . All structures were solved by direct methods. In the crystal lattice of **3**, there is a toluene solvent molecule residing on an inversion center. As a result, the toluene molecule is disordered over two sites related by the inversion center. The methyl group of the toluene could not be located. All non-hydrogen atoms were refined anisotropically. The positions for all hydrogen atoms except those attached to the disordered solvent molecule were calculated, and their contributions in structural factor calculation were included. The crystals of compound **4** are of marginal quality, which could account for the relatively poor structural data of **4**. The crystallographic data for compounds **1–4** are given in Table 1.

**Syntheses and Structures of Di-2-pyridylamine Complexes.** Al(CH<sub>3</sub>)<sub>2</sub>(dpa) (**1**). When Al(CH<sub>3</sub>)<sub>3</sub> was reacted with di-2-pyridylamine in a 1:1 ratio under a carefully controlled oxygen-free environment at 23 °C and in toluene, the pale yellow colored compound **1**, Al(CH<sub>3</sub>)<sub>2</sub>(dpa), was obtained in good yield. Compound **1** is highly air-sensitive. Its composition and structure were established by <sup>1</sup>H NMR spectroscopy and elemental and X-ray diffraction analyses. Selected bond lengths and angles are listed in Table 2. As shown in Figure 1, the dpa ligand chelates to the aluminum center through the two pyridyl nitrogen atoms. The aluminum atom is in a tetrahedral environment with normal Al–N and Al–C bond lengths.<sup>8,11,13</sup> The amido nitrogen atom, N(3), is negatively charged due to the loss of the proton. As a result, compound **1** is a zwitterion. The dpa ligand is essentially planar (the

dihedral angle between the two pyridyl rings is 7.3°). The Al(1) ion is essentially coplanar with the dpa plane, while the two methyl groups on Al(1) are situated nearly symmetrically with respect to the dpa plane. The structure of compound **1** is an analogue<sup>12</sup> of Ga(CH<sub>3</sub>)<sub>2</sub>(dpa). A few mononuclear dialkyl-aluminum complexes with a tetrahedral AlC<sub>2</sub>N<sub>2</sub> core structure have been reported previously.<sup>8d,13</sup>

Al<sub>2</sub>(CH<sub>3</sub>)<sub>5</sub>(dpa) (**2**). In compound **1**, the amido nitrogen atom N(3) has two lone pairs of electrons and is not bound to the metal center. One can therefore anticipate that it is possible to incorporate an additional metal center into the complex by utilizing the N(3) binding site. Indeed, when Al(CH<sub>3</sub>)<sub>3</sub> was reacted with di-2-pyridylamine in a 2:1 ratio under N<sub>2</sub> at 23 °C in toluene, colorless block crystals of compound **2**, formulated as Al<sub>2</sub>(CH<sub>3</sub>)<sub>5</sub>(dpa), were obtained in good yield. The structure of compound **2** was determined by X-ray diffraction analysis. Selected bond lengths and angles are given in Table 2. There are two independent molecules of **2** in the asymmetric unit with essentially identical bond lengths and angles. The structure of one of the independent molecules is shown in Figure 2. One of the aluminum centers, Al(1) (an Al(CH<sub>3</sub>)<sub>2</sub> moiety), in **2** is chelated by the dpa ligand in the same fashion as that in **1**. The second aluminum center, Al(2) (an Al(CH<sub>3</sub>)<sub>3</sub> moiety), is attached to the amido N(3) atom, as anticipated. Unlike in compound **1** where the dpa ligand and the Al(1) atom are coplanar, the dpa ligand in **2** is puckered with a 30.7° dihedral angle between the two pyridyl rings. As a result, the two methyl groups on Al(1) have distinct chemical environments (Figure 2): one orients toward the Al-(CH<sub>3</sub>)<sub>3</sub> moiety, while the other is away from it. The loss of coplanarity between the dpa ligand, Al(1), and Al(2) in **2** is most likely caused by steric interactions among the hydrogen atoms of methyl and dpa ligands in the solid state. If compound **2** retains the same structure in solution, one would expect to see three methyl resonances in a 3:1:1 ratio in its <sup>1</sup>H NMR spectrum: one from the Al(CH<sub>3</sub>)<sub>3</sub> group and two from the Al(CH<sub>3</sub>)<sub>2</sub> group. However, at ambient temperature, only two methyl resonances in a 3:2 ratio were observed. When the temperature was lowered (298 K to 213 K), the signal corresponding to Al(CH<sub>3</sub>)<sub>2</sub> became increasingly broader, while the Al(CH<sub>3</sub>)<sub>3</sub> signal remained sharp, an indication that the two methyl groups on Al(1) undergo a facile exchange process in solution. The <sup>13</sup>C NMR spectrum of **2** at 213 K shows three distinct chemical shifts of Al–CH<sub>3</sub>, indicating that at low temperature the structure of **2** in solution is the same as that in the solid state. The exchange process could be explained by a rapid fluctuation between two puckered six-membered rings consisting of Al(1), N(1), N(2), N(3), C(7), and C(8), which

(10) Cromer, D. T.; Waber, J. T. *International Tables for X-ray Crystallography*; Kynoch Press: Birmingham, AL, 1974; Vol. 4, Table 2.2A.

(11) Mole, T.; Jeffrey, E. A. *Organoaluminum Compounds*; Elsevier: New York, 1972. (b) Lappert, M. F.; Power, P.; Sanger, A. R.; Srivastava, R. C. *Metal and Metalloid Amides*; Ellis Horwood/Wiley: New York, 1980. (c) Cesari, M.; Cucinella, S. Aluminum–Nitrogen Rings and Cages. In *The Chemistry of Inorganic Homo and Heterocycles*; Haiduc, I., Sowerby, B., Eds.; Academic Press: London, 1987. (d) Janik, J. F.; Duesler, E. N.; Paine, R. T. *Inorg. Chem.* **1988**, *27*, 4335. (e) Janik, J. F.; Duesler, E. N.; Paine, R. T. *Inorg. Chem.* **1987**, *26*, 4341.

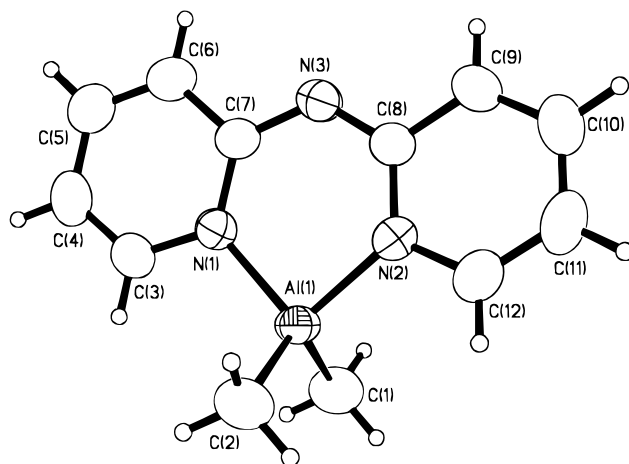
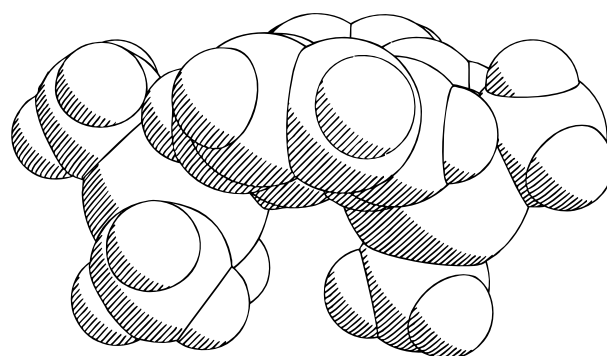
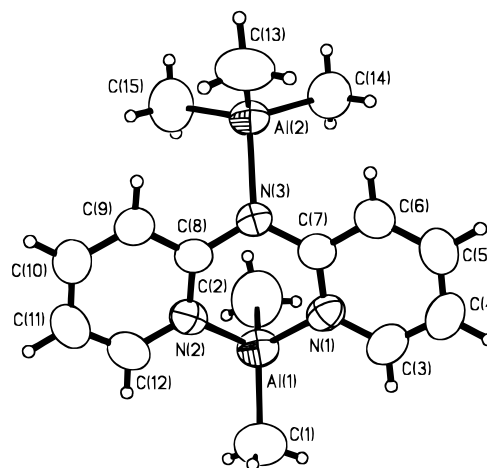
(12) Wang, X.; Sun, H.; You, X. *Polyhedron* **1996**, *15*, 3543. The synthesis of Al(CH<sub>3</sub>)<sub>2</sub>(dpa) was described in the same article, but no crystal structural data were reported.

(13) Beachley, O. T., Jr.; Racette, K. C. *Inorg. Chem.* **1976**, *15*, 2110; **1975**, *14*, 2534. (b) Hasselbring, R.; Rpesky, H. W.; Heine, A.; Stalke, D.; Sheldrick, G. M. *Z. Naturforsch.* **1994**, *49B*, 43.



**Table 2. Selected Bond Lengths [Å] and Angles [deg]**

Compound 1			
Al(1)–N(1)	1.919(2)	N(1)–C(3)	1.377(3)
Al(1)–N(2)	1.922(2)	N(2)–C(8)	1.369(3)
Al(1)–C(2)	1.949(3)	N(2)–C(12)	1.370(3)
Al(1)–C(1)	1.954(3)	N(3)–C(8)	1.346(3)
N(1)–C(7)	1.365(3)	N(3)–C(7)	1.348(3)
N(1)–Al(1)–N(2)	93.85(9)	N(2)–Al(1)–C(1)	110.74(11)
N(1)–Al(1)–C(2)	111.33(11)	C(2)–Al(1)–C(1)	116.78(14)
N(2)–Al(1)–C(2)	111.59(12)	C(8)–N(3)–C(7)	126.2(2)
N(1)–Al(1)–C(1)	110.24(12)		
Compound 2			
Al(1)–N(1)	1.924(3)	Al(3)–N(6)	2.010(2)
Al(1)–N(2)	1.926(3)	N(3)–C(8)	1.382(3)
Al(1)–C(2)	1.938(4)	N(3)–C(7)	1.384(3)
Al(1)–C(1)	1.944(4)	Al(4)–N(4)	1.926(3)
N(1)–C(7)	1.352(3)	Al(4)–N(5)	1.926(2)
N(1)–C(3)	1.360(4)	Al(4)–C(16)	1.941(4)
Al(2)–C(15)	1.969(4)	Al(4)–C(17)	1.951(3)
Al(2)–C(14)	1.987(4)	N(4)–C(22)	1.361(3)
Al(2)–C(13)	1.996(5)	N(4)–C(18)	1.362(4)
Al(2)–N(3)	2.011(2)	N(5)–C(23)	1.353(3)
N(2)–C(8)	1.349(3)	N(5)–C(27)	1.357(4)
N(2)–C(12)	1.355(4)	C(5)–C(6)	1.364(4)
Al(3)–C(30)	1.976(4)	N(6)–C(23)	1.376(3)
Al(3)–C(29)	1.978(4)	N(6)–C(22)	1.380(3)
Al(3)–C(28)	1.979(4)		
N(1)–Al(1)–N(2)	90.52(10)	C(29)–Al(3)–C(28)	112.2(2)
N(1)–Al(1)–C(2)	108.9(2)	C(30)–Al(3)–N(6)	105.01(14)
N(2)–Al(1)–C(2)	109.4(2)	C(29)–Al(3)–N(6)	107.35(14)
N(1)–Al(1)–C(1)	110.6(2)	C(28)–Al(3)–N(6)	106.54(13)
N(2)–Al(1)–C(1)	110.3(2)	C(8)–N(3)–C(7)	121.7(2)
C(2)–Al(1)–C(1)	122.4(2)	N(4)–Al(4)–N(5)	90.21(10)
C(15)–Al(2)–C(13)	114.8(2)	N(4)–Al(4)–C(16)	110.7(2)
C(14)–Al(2)–C(13)	113.5(2)	N(5)–Al(4)–C(16)	108.9(2)
C(15)–Al(2)–N(3)	106.0(2)	N(4)–Al(4)–C(17)	110.0(2)
C(14)–Al(2)–N(3)	106.69(14)	N(5)–Al(4)–C(17)	110.83(14)
C(13)–Al(2)–N(3)	105.6(2)	C(16)–Al(4)–C(17)	121.7(2)
C(30)–Al(3)–C(29)	114.2(2)	C(23)–N(6)–C(22)	121.1(2)
C(30)–Al(3)–C(28)	110.9(2)		
Compound 3			
Al(1)–O'	1.797(3)	Al(2)–N(2)	1.985(3)
Al(1)–O	1.870(2)	N(1)–C(9)	1.367(4)
Al(1)–C(1)	1.971(4)	N(1)–C(8)	1.383(4)
Al(1)–N(1)	1.998(3)	N(2)–C(13)	1.348(4)
Al(1)–N(3)	2.149(3)	N(2)–C(9)	1.371(4)
Al(2)–O	1.768(2)	N(3)–C(4)	1.330(5)
Al(2)–C(2)	1.953(4)	N(3)–C(8)	1.344(5)
Al(2)–O–Al(1')	140.3(2)	O–Al(1)–N(3)	156.18(12)
Al(2)–O–Al(1)	116.51(13)	C(1)–Al(1)–N(3)	94.4(2)
Al(1')–O–Al(1)	95.22(11)	N(1)–Al(1)–N(3)	63.75(12)
O'–Al(1)–O	84.78(11)	C(9)–N(1)–C(8)	123.9(3)
O'–Al(1)–C(1)	118.8(2)	O–Al(2)–C(3)	115.0(2)
O–Al(1)–C(1)	104.3(2)	O–Al(2)–C(2)	113.7(2)
O'–Al(1)–N(1)	114.81(12)	C(3)–Al(2)–C(2)	114.1(2)
O–Al(1)–N(1)	93.15(12)	O–Al(2)–N(2)	99.24(12)
C(1)–Al(1)–N(1)	124.6(2)	C(3)–Al(2)–N(2)	106.7(2)
O'–Al(1)–N(3)	99.23(12)	C(2)–Al(2)–N(2)	106.2(2)
Compound 4			
Al(1)–N(1)	2.025(7)	N(3)–C(12)	1.315(10)
Al(1)–N(2)	1.960(7)	N(3)–C(16)	1.377(11)
Al(1)–N(3)	2.035(8)	N(4)–C(16)	1.336(10)
Al(1)–N(4)	1.958(7)	N(4)–C(17)	1.385(10)
Al(1)–N(5)	2.015(7)	N(5)–C(23)	1.327(10)
Al(1)–N(6)	1.952(7)	N(5)–C(27)	1.363(10)
N(1)–C(5)	1.350(10)	N(6)–C(27)	1.378(10)
N(2)–C(6)	1.386(10)	N(6)–C(28)	1.411(10)
N(2)–C(5)	1.358(10)		
N(6)–Al(1)–N(4)	101.5(3)	N(5)–Al(1)–N(1)	97.0(3)
N(6)–Al(1)–N(2)	102.4(3)	N(6)–Al(1)–N(3)	157.2(3)
N(4)–Al(1)–N(2)	101.9(3)	N(4)–Al(1)–N(3)	66.9(3)
N(6)–Al(1)–N(5)	66.7(3)	N(2)–Al(1)–N(3)	99.3(3)
N(4)–Al(1)–N(5)	97.3(3)	N(5)–Al(1)–N(3)	94.5(3)
N(2)–Al(1)–N(5)	159.6(3)	N(1)–Al(1)–N(3)	97.9(3)
N(6)–Al(1)–N(1)	97.1(3)	C(5)–N(2)–C(6)	123.4(7)
N(4)–Al(1)–N(1)	159.9(3)	C(16)–N(4)–C(17)	122.6(7)
N(2)–Al(1)–N(1)	66.4(3)	C(27)–N(6)–C(28)	124.7(7)

**Figure 1.** Diagram showing the molecular structure of **1** with 50% thermal ellipsoids.**Figure 2.** Diagram showing the molecular structure of **2** with 50% thermal ellipsoids (top) and a space-filling diagram showing the side view of **2** (bottom).

averages the chemical environments of the two methyl groups. A similar exchange process has been observed previously.<sup>8d</sup>

**Al<sub>4</sub>(CH<sub>3</sub>)<sub>6</sub>(μ<sub>3</sub>-O)<sub>2</sub>(dpa)<sub>2</sub> (**3**).** Compounds **1** and **2** are highly air-sensitive. To improve the stability of the complex, we explored the possibility of incorporating oxo, hydroxyl, or alkoxy ligands into the dpa aluminum complexes. By simply including alcohol or water in the reaction mixture, we were able to isolate several interesting and relatively stable oxo and alkoxy aluminum complexes based on 7-azaindole and its derivatives.<sup>5a,6</sup> This strategy has not however been very successful with the dpa-based complexes. The only compound that we have been able to isolate successfully is compound **3**,

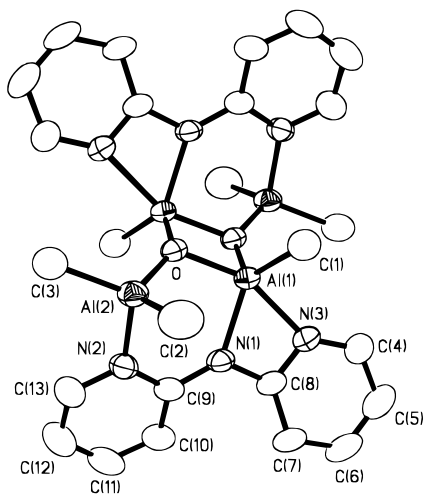


**Figure 3.** Diagram showing the molecular structure of **3** with 50% thermal ellipsoids. Hydrogen atoms are omitted for clarity.

obtained in 50% yield by the reaction of dpaH with 2 equiv of  $\text{Al}(\text{CH}_3)_3$  in the presence of  $\text{H}_2\text{O}$  (the water molecules could be introduced either by using a small amount of unpurified solvent such as dmf or by carrying out the reaction under a water-vapor-saturated nitrogen atmosphere) in toluene at 23 °C. Compound **3** was fully characterized by  $^1\text{H}$  NMR spectroscopy, single-crystal X-ray diffraction, and elemental analyses. Selected bond lengths and angles are listed in Table 2. The structure of **3** is shown in Figure 3. (The structure of **3** has been described in a preliminary communication article.<sup>5a</sup>)

Compound **3** contains four Al atoms and an inversion center symmetry as shown in Figure 3. In compound **2**, the pyridyl groups and the amido nitrogen atom are bound to two different aluminum centers, respectively. In contrast, one pyridyl group N(3) and the amido nitrogen atom N(1) are bound to the same aluminum, Al(1), in **3**, while the remaining pyridyl N(2) atom is bound to Al(2). The Al(1)–N(1) (amido) bond length (1.998(3) Å) is somewhat shorter than that of Al(1)–N(3) (pyridyl, 2.149(3) Å), probably due to the relatively high affinity of the negatively charged amido nitrogen atom toward the Al(III) ion. The three methyl groups, C(1), C(2), and C(3), have different chemical environments: C(1) is bound to Al(1), while C(2) and C(3) are bound to Al(2) with C(2) being *cis* to C(1). Compound **3** retains its structure in solution as confirmed by the three distinct methyl resonances in the  $^1\text{H}$  NMR spectrum of **3** at 298 K. The oxo ligand, produced by the reaction of one  $\text{H}_2\text{O}$  with two methyl ligands, bridges three aluminum centers with an approximately pyramidal geometry (the oxygen atom is 0.280 Å above the Al(1)Al(1a)Al(2) plane). A similar bonding mode of the oxo ligand has been reported in complexes<sup>14</sup>  $[(\text{CH}_3)_2\text{Al}(\mu_3\text{-O})\text{Al}(\text{CH}_3)_3]_2^{2-}$ ,  $[\text{Al}_3(\mu_3\text{-O})\text{Cl}_8]^-$ , and  $[\text{AlCl}_2(\mu_3\text{-O})(\text{AlCl}_3)]_2^{2-}$ . The Al–O bond lengths are in the normal range of the known Al–O bond lengths.<sup>14,15</sup> The Al(1)–Al(1') separation distance is 2.708(2) Å. The geometry of the Al(1) atom can be described as that of a distorted trigonal bipyramid, with N(3) and O on the axial positions, while the geometry of the Al(2) ion is tetrahedral. The dpa ligand in **3** is not planar, with a dihedral angle between the two pyridyl

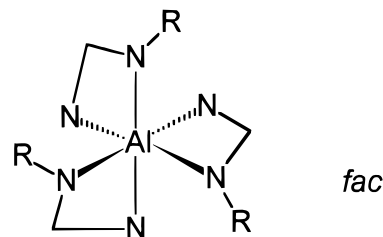
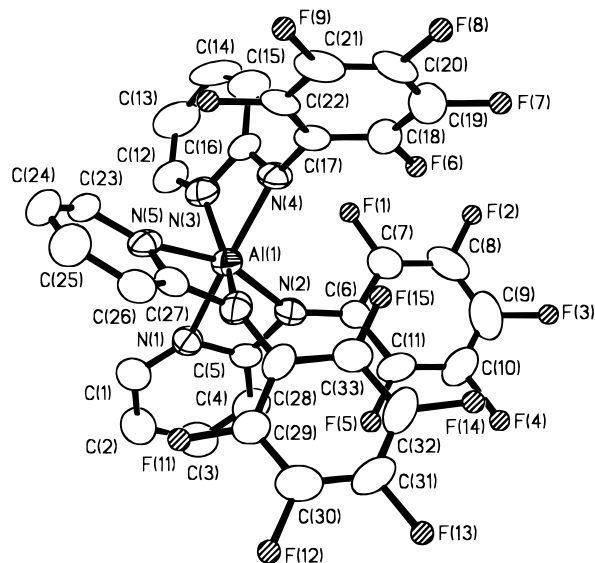


**Figure 4.** (Top) Diagram showing the molecular structure of **4** with 50% thermal ellipsoids. Hydrogen atoms are omitted and the fluorine atoms are shown as ideal spheres for clarity. (Bottom) Line drawing diagram showing the *fac* structure of **4**, R =  $\text{C}_6\text{F}_5$ .

rings being 30.0°, similar to that in **2**. In comparison to the highly air-sensitive compounds **1** and **2**, compound **3** is stable for a few hours in the solid state upon exposure to air, which is attributable to the presence of the oxo ligands.

**Syntheses and Structures of the 2-Pentafluoroanilino-pyridine Complex,  $\text{Al}(\text{pfap})_3$  (**4**).** The dpa ligands in compounds **1–3** are all anions with the negative charge centered on the amido nitrogen atom. As a result, the dpa ligand is also susceptible to moisture (producing the neutral ligand, dpaH) just like the methyl group (producing methane). One way to improve the stability of the coordinated dpa ligand is to reduce the negative charge on the amido nitrogen atom so that it is less susceptible to moisture. The introduction of oxo ligands in complex **3** appeared to stabilize the dpa ligand. Alternatively, one could replace one of the pyridyl rings of the dpa with an electron-withdrawing group such as pentafluorophenyl to reduce the charge density on the amido nitrogen without losing the luminescence. We therefore synthesized the 2-pentafluoroanilinopyridine (pfapH) ligand. Only one compound was isolated from the reaction of  $\text{Al}(\text{CH}_3)_3$  with pfapH in toluene, namely,  $\text{Al}(\text{pfap})_3$  (**4**). Compound **4** can be obtained readily in high yield by the stoichiometric reaction of  $\text{Al}(\text{CH}_3)_3$  with pfapH. As shown in Figure 4, the aluminum ion in **4** is in an approximately octahedral environment. There are two possible geometric isomers for compound **4**, *facial* and *meridional*.<sup>16</sup> In the solid state, the structure of compound **4** is *fac* (Figure 4) because each pyridyl group is approximately *trans* to the pentafluoroanilino group as shown by the angles of N(1)–Al(1)–N(4) (159.9(3)°), N(3)–Al(1)–N(6) (157.2(3)°), and N(5)–Al(1)–N(2) (159.6(3)°). The distortion of compound **4** from an ideal octahedral geometry can be attributed to the

(14) Atwood, J. L.; Zaworotko, M. J. *J. Chem. Soc., Chem. Commun.* **1983**, 302. (b) Thewalt, U.; Stollmaier, F. *Angew. Chem., Int. Ed. Engl.* **1982**, *21*, 133.

(15) Laussac, J.-P.; Enjalbert, R.; Galy, J.; Laurent, J. P. *J. Coord. Chem.* **1983**, *12*, 133. (b) Chisholm, M. H.; Distasi, V. F.; Streib, W. E. *Polyhedron* **1990**, *9*, 253. (c) Trepanier, S. J.; Wang, S. *Angew. Chem., Int. Ed. Engl.* **1994**, *33*, 1265. (d) Robinson, G. H.; Lee, B.; Pennington, W. T.; Sangokoya, S. A. *J. Am. Chem. Soc.* **1988**, *110*, 6260. (e) Self, M. F.; Pennington, W. T.; Laske, J. A.; Robinson, G. H. *Organometallics* **1991**, *10*, 36. (f) Sango, S. A.; Pennington, W. T.; Byers-Hill, J.; Robinson, G. H. *Organometallics* **1993**, *12*, 2429.

(16) Cotton, F. A.; Wilkinson, G. *Advanced Inorganic Chemistry*, 5th ed.; John Wiley & Sons: New York, 1988.

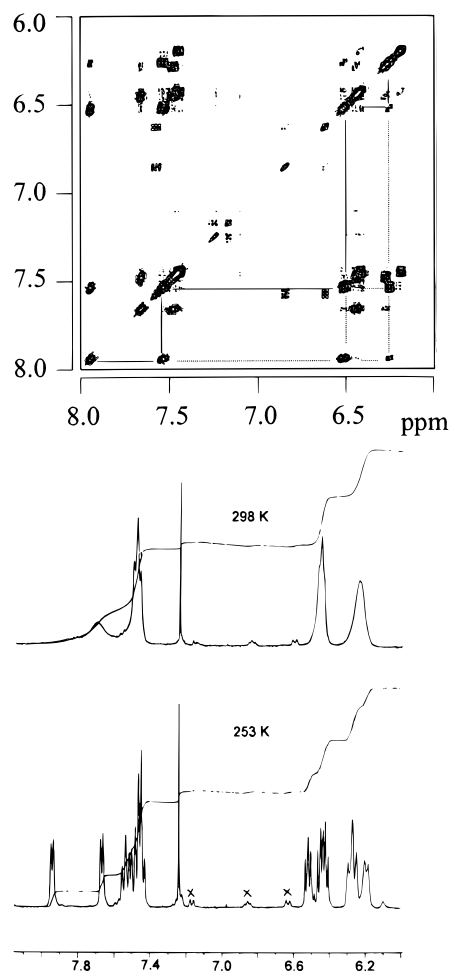


**Figure 5.** (Top) 2D  $^1\text{H}$  COSY spectrum of **4** obtained at 243 K in  $\text{CDCl}_3$ . For clarity only one of the three sets of cross-peaks are labeled. Solid lines indicate cross-peaks due to  $^3J$  couplings, whereas the dash lines indicate those from long-range couplings. (Bottom)  $^1\text{H}$  NMR spectra of compound **4** in  $\text{CDCl}_3$ . The impurity peaks are marked by "X".

small bite angle of the pfap ligand. A similar distorted octahedral geometry has been observed in  $\text{Al}(1,3\text{-diaryltriazenido})_3$  complexes reported by Barron and co-workers<sup>17a,b</sup> and  $\text{Al}(\text{dpa})_3$  reported by Raston and co-workers.<sup>17c</sup> The  $\text{Al}(1)\text{-amido}$  nitrogen bond lengths ( $\text{Al}(1)\text{-N}(2)$ ,  $\text{Al}(1)\text{-N}(4)$ , and  $\text{Al}(1)\text{-N}(6)$ ) are consistently shorter than those of  $\text{Al}(1)\text{-pyridyl}$  nitrogen bonds ( $\text{Al}(1)\text{-N}(1)$ ,  $\text{Al}(1)\text{-N}(3)$ , and  $\text{Al}(1)\text{-N}(5)$ ), again attributable to the relatively high affinity of the amido nitrogen atom toward the aluminum ion. The pentafluorophenyl portion of the pfap ligand is not coplanar with the pyridyl ring, attributable to steric interactions. Compound **4** is fairly stable under air in the solid state, attributable to the absence of methyl ligands and the presence of the electron-withdrawing pentafluorophenyl group.

If compound **4** retains the *fac* geometry in solution, it should have an approximate  $C_3$  symmetry. Consequently, only one set of pyridyl resonances (four resonances in a 1:1:1:1 ratio) should be observed in the  $^1\text{H}$  NMR spectrum. At 298 K, one set of broad pyridyl resonances were indeed observed. However, as the temperature was lowered, the spectral pattern became more complex (Figure 5, bottom). At  $-20^\circ\text{C}$ , eight groups of resonances of pyridyls with the relative integral ratio of 1:1:1:3:1:2:2:1 were observed. Further decreasing the temperature caused no significant change in the spectrum. If

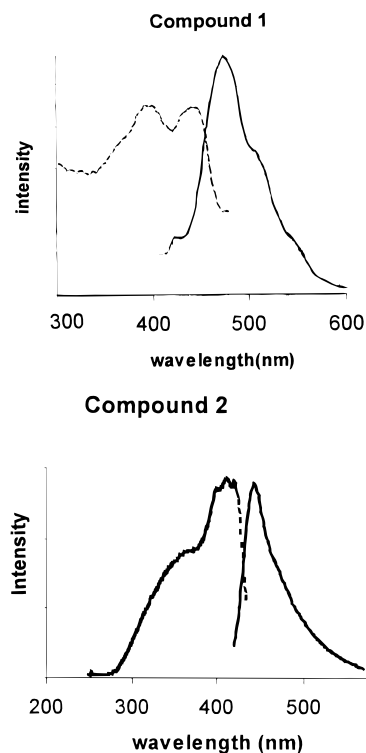


**Figure 6.** Excitation and emission spectra of **1** and **2**.

compound **4** has the *mer* structure in solution, all three pyridyl groups are chemically inequivalent, which would in principle result in 12 resonances with equal integrated intensities in the  $^1\text{H}$  NMR spectrum. The low-temperature  $^1\text{H}$  NMR spectrum could be therefore attributed entirely to the *mer* isomer. The fact that eight resonances, instead of 12, were observed can be explained by accidental overlaps of some of the resonances. To confirm it, we carried out a 2D COSY  $^1\text{H}$  NMR experiment at 243 K. The 2D COSY  $^1\text{H}$  spectrum of **4** (Figure 5, top) shows clearly three sets of cross-peaks, indicating that the three pfap ligands in **4** are nonequivalent in solution and the *mer* isomer is indeed favored at low temperature. The *mer* isomer is clearly thermodynamically more stable than the *fac* isomer, perhaps due to steric reasons. The fact that only the *fac* isomer was found in the solid state could be explained by the relatively favorable packing of **4** in the crystal lattice, which results in the formation of single crystals suitable for X-ray diffraction analysis. It is very likely that the bulk of the solid sample of **4** contains both *mer* and *fac* isomers. The poor quality of *mer* crystals may be the reason that the *mer* structure was not determined. Solid-state NMR experiments could provide a conclusive answer to the existence of the *mer* isomer in the solid state and will be investigated by our group. A fluxional behavior has also been observed in the  $\text{Al}(\text{dpa})_3$  complex reported by Raston,<sup>17c</sup> but the cause of the fluxionality displayed by  $\text{Al}(\text{dpa})_3$  has not been conclusively established.

**Luminescent Properties of Compounds 1–4.** The free ligand  $\text{dpaH}$  has no emission in the visible region in solution and has a very weak emission at  $\lambda = 420$  nm (purple-blue), hardly visible by eye, in the solid state, when irradiated by UV light. Compounds **1–3**, in contrast, yield intense luminescence when irradiated by UV light in solution and the solid state. In the solid state compound **1** emits  $\lambda = 475$  nm (greenish blue), while compounds **2** and **3** emit at  $\lambda = 445$  and  $450$  nm (royal blue), respectively (Figures 6 and 7). The solution luminescent spectra of compounds **1–3** are similar to those of solids. The consequence of formation of the  $\text{dpa}$  complexes appears to be 2-fold. First, the emission energy is shifted to longer wavelengths (more blue). Second, the emission becomes more efficient, as indicated by the brighter emission of compounds **1–3** in the solid state, in comparison

(17) Leman, J. T.; Barron, A. R.; Ziller, J. W.; Kren, R. M. *Polyhedron* **1989**, *8*, 1909. (b) Leman, J. T.; Braddock-Wilking, J.; Coolong, A. J.; Barron, A. J. *Inorg. Chem.* **1993**, *32*, 4324.



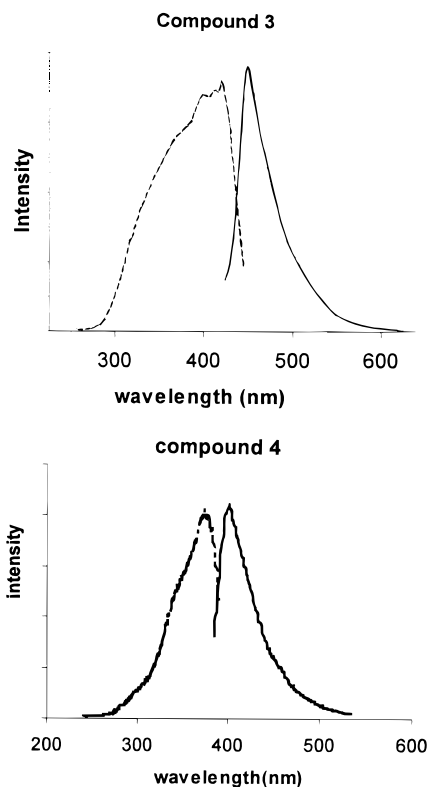


**Figure 7.** Excitation and emission spectra of **3** and **4**.

to that of dpaH. The quantum yield of emission in solution for compound **3** was determined to be 0.37, relative to that of 9,10-diphenylanthracene in cyclohexane,<sup>18</sup> evidence that compound **3** is indeed a good emitter in solution. The enhanced emission efficiency in the complexes could be attributed to the chelating of the dpa ligand to the aluminum ion that effectively increases the rigidity of the ligand and reduces the loss of energy via radiationless thermal vibrations.<sup>19</sup> The quantum yields for compounds **1** and **2** were not measured because of their poor stability in solution. Ideally one should measure the emission quantum yield of the solid because the solid luminescence is related directly to electroluminescence.<sup>3c</sup> Unfortunately, the measurement of emission quantum yields of solids is a very time-consuming and challenging task. We therefore did not measure the quantum yield of our compounds in the solid state. The emission lifetime of compound **3** was determined to be 5.0 ns, consistent with a fluorescent emission.

The blue luminescence exhibited by compounds **1–3** is believed to originate from a  $\pi^* \rightarrow \pi$  transition localized on the dpa ligand. The common feature in compounds **1–3** is that the dpa ligand is deprotonated, which may play a key role in shifting the emission energy to longer wavelengths. From the crystal structures, it is evident that the conjugation of both pyridyl rings with the amido nitrogen is not necessary for the blue luminescence since such conjugation does not exist in compounds **2** and **3**. To understand the role of the aluminum ion in the luminescence of compounds **1–3**, we carried out a molecular orbital calculation on the free ligand, dpaH, the deprotonated ligand, dpa, and compound **1** by using *ab initio*

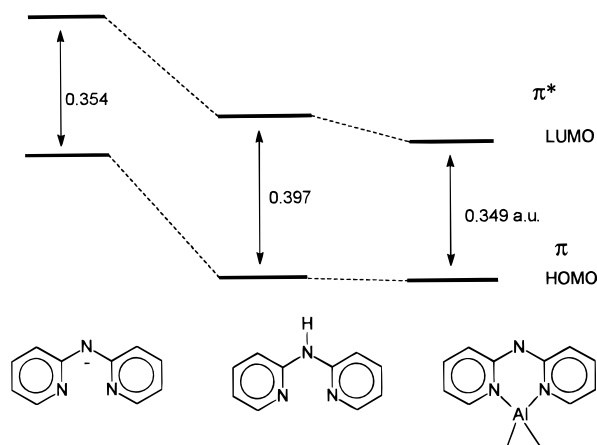


**Figure 8.** Diagram showing the HOMO and LUMO energy levels of the dpa anion, the free dpaH ligand, and compound **1**.

methods<sup>20</sup> (Gaussian 94, basis set 6-31G\*/RHF) and geometric parameters from crystal structural data. The HOMO orbitals for all three compounds are  $\pi$  bonding orbitals, while the LUMO orbitals are  $\pi$  antibonding orbitals for all compounds. The HOMO–LUMO gaps for the dpa anion, the free ligand, dpaH, and compound **1** are 0.356, 0.397, and 0.349 au, respectively (Figure 8). The HOMO–LUMO gaps for the dpa anion and compound **1** are similar, consistent with the fact that Li(dpa) and Na(dpa) also emit in the same energy region as compound **1** does.<sup>21</sup> The overall energy of the dpa anion is however much higher than that of compound **1**, which makes us conclude that one of the roles played by the aluminum ion is to stabilize the dpa anion by accepting lone pairs of electrons from the dpa ligand, thus lowering the HOMO and LUMO levels. The HOMO–LUMO gap of the neutral dpaH ligand is however significantly larger than those of the dpa anion and compound **1**, consistent with the fact that the free dpaH ligand emits at a shorter wavelength (420 nm in the solid state) than the dpa anion and compound **1** do (>450 nm). The major difference between the dpaH ligand and compound **1** is that the LUMO of compound **1** is lower in energy than that of dpaH, attributable to the mixing of aluminum atomic orbitals in the LUMO of **1** that stabilizes the LUMO. On the basis of the calculation results, we can conclude that the blue luminescence exhibited by compound **1** can be attributed to two factors. First, the removal of the proton from the dpaH ligand decreases the HOMO–LUMO gap largely due to the destabilization of the HOMO by the negative charge so that the dpa anion emits at a longer wavelength than that of dpaH. Second, the formation of complex between the aluminum ion and the dpa anion stabilizes the dpa anion by stabilizing both HOMO and LUMO orbitals but does not significantly alter the HOMO–LUMO gap, so that the complex still emits at a longer wavelength than that of dpaH. A similar phenomenon was also observed in blue luminescent 7-azaindole-based aluminum complexes.<sup>6</sup> Although we did not perform *ab initio* calculations on compounds **2** and **3** because of their large sizes, there is no doubt that the aluminum ion plays the same roles in **2** and **3** as it does in **1**, i.e., stabilizing the dpa anion.

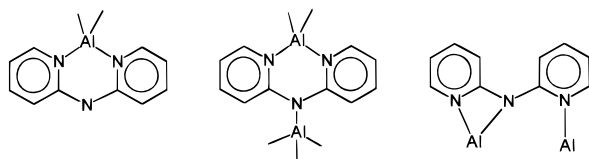
In contrast to the 7-azaindole-based polynuclear aluminum complexes reported previously,<sup>6</sup> where the emission energy of the complexes changes little with the change of the nonemitting ligand environment around the aluminum, there is a significant change of emission energy from compound **1** (475 nm) to compound **3** (450 nm). The difference between **1**, **2**,

(18) Demas, J. N.; Crosby, G. A. *J. Phys. Chem.* **1971**, *75*, 991. (b) Engelhardt, L. M.; Gardiner, M. C.; Jones, C.; Junk, P. C.; Raston, C. L.; White, A. H. *J. Chem. Soc., Dalton Trans.* **1996**, 3053.

(19) *Fluorescence and Phosphorescence*; Rendell, D., Ed.; John Wiley & Sons: New York, 1987. (b) *Photochemistry and Photophysics of Coordination Compounds*; Yersin, H.; Vogler, A., Eds.; Springer-Verlag: Berlin, 1987. (c) *Concepts of Inorganic Photochemistry*; Adamson, A. W.; Fleischauer, P. D., Eds.; John Wiley & Sons: New York, 1975.

(20) *Gaussian 94*, Revision B.3; Gaussian, Inc.: Pittsburgh, PA, 1995.

(21) The reaction of butyllithium or NaH with di-2-pyridylamine also yields an intense blue luminescent compound, Li(dpa) or Na(dpa). These compounds are however highly unstable.

**Chart 2. Bonding Modes Exhibited by the dpa Ligand in 1–3**

and **3** could be explained by the different bonding modes of the dpa ligand (Chart 2). (In comparison, all 7-azaindole ligands in our polynuclear aluminum complexes exhibit only one bridging bonding mode.<sup>6</sup>) In **1**, the two pyridyl rings are bound to one Al(III) in a coplanar fashion, while in **2** and **3** not only is the amido nitrogen atom also bound to Al(III) but, more importantly, the dpa ligand is no longer coplanar. The loss of coplanarity of the dpa ligand certainly would decrease the degree of  $\pi$  conjugation, which in turn can result in the increase of HOMO–LUMO gap ( $\pi$ – $\pi^*$  gap) and lead to the emission energy shift to a shorter wavelength. The lack of coplanarity of the dpa ligand in **2** and **3** leads us to believe that the conjugation of 2-amido nitrogen with one pyridyl ring, albeit shifting the emission energy to a shorter wavelength than that of **1**, is sufficient to produce a blue luminescence. In fact we have observed that the reaction mixture of  $\text{Al}(\text{CH}_3)_3$  with 2-aminopyridine yielded a similar blue luminescence as those of **2** and **3**, a further indication that the 2-amidopyridine portion is the key to blue luminescence.<sup>22</sup>

Although compounds **1–3** are blue luminescent, their applications in electroluminescence are however hampered by the poor stability of **1** and **2** and the low volatility of **3**. (Compound **3** has a melting point of 165 °C and could not be sublimed at 0.1 mmHg and <165 °C.) The replacement of one of the pyridyl rings in dpa by a pentafluorophenyl ring, albeit yielding a stable complex **4**, shifts the emission energy to near UV, which is somewhat disappointing but not surprising. As shown in Figure 8, the emission maximum of compound **4** (409 nm, purple) is at a much shorter wavelength than those of compounds **1–3**. Because the pentafluorophenyl group is a much better electron-withdrawing group than pyridyl, it can effectively decrease the electron density on the amido nitrogen atom, thus reducing the energy of the HOMO level and leading to a larger HOMO–LUMO gap than those of dpa complexes. Compound **4** has a high melting point (>280 °C) and is stable for several days upon exposure to air in the solid state.

(22) At this time, we have not yet been able to isolate any crystalline products from the reaction of  $\text{Al}(\text{CH}_3)_3$  with 2-aminopyridine to establish the structures of 2-aminopyridine complexes. This work is still in progress.

Although compound **4** is not blue luminescent, it may find use in electroluminescence due to its high emission energy.<sup>3</sup> Unfortunately, our attempts to sublime compound **4** under our laboratory conditions (0.1 mmHg, 240 °C) have not been successful.

## Conclusion

The complexation of the deprotonated di-2-pyridylamine to an aluminum ion results in new blue luminescent compounds. The blue luminescence of the dpa complexes could be attributed to a  $\pi \rightarrow \pi$  transition of the dpa ligand. The key  $\pi$  conjugation for yielding the blue luminescence appeared to be the 2-amidopyridine portion of the dpa ligand. The role of the aluminum ion in the dpa complexes appeared to be at least 2-fold: (1) stabilizing the dpa anion by accepting the lone pairs of electrons from the ligand; (2) reducing the thermal vibrations of the dpa ligand by chelating to the dpa ligand, thus enhancing the emission efficiency. The new blue luminescent dpa complexes may not have any practical value in electroluminescent display due to their poor stability or low volatility, but they provide new insight into the design and development of new blue luminescent complexes. The replacement of one of the pyridyl rings in the dpa ligand by a pentafluorophenyl group leads to the formation of a stable complex  $\text{Al}(\text{p-fap})_3$  (**4**), with the emission energy being shifted toward near the UV region. Compound **4** is not a blue emitter, but it may find use in electroluminescent devices due to its high emission energy.

**Acknowledgment.** We thank NSERC of Canada for financial support, Dr. Linda Johnston (NRC) for providing the instruments for quantum yield and emission lifetime measurements, and Professor Steven Brown and Samir Tabash for assistance in recording excitation and emission spectra.

**Supporting Information Available:** Tables of crystallographic analysis data, atomic coordinates, and isotropic thermal parameters, a complete list of bond lengths and angles, anisotropic thermal parameters, hydrogen parameters, and a diagram showing the disordered toluene molecule in the lattice of **3** (19 pages). Ordering information is given on any current masthead page.

OM980536H